Electronic Supplementary Material (ESI) for Dalton Transactions.
This journal is © The Royal Society of Chemistry 2024

Experimental Section/Methods

Materials and characterizations: nickel chloride hexahydrate ($NiCl_2·6H_2O$), ammonium hydroxide ($(NH_4)_6Mo_7O_{24}·4H_2O$), citric acid monohydrate ($C_6H_5Na_3O_7$), sodium carbonate (Na_2CO_3) and potassium hydroxide (KOH) were purchased from Aladdin Ltd. All chemicals are analytical reagent graded and used as received without further purification.

Synthesis of the POMs-Ni@PTM: The electrodeposition is performed in a three-electrode glass cell by using CS350 (Wuhan Corrtest Instruments Corp. Ltd.) electrochemical working station. The porous Ti mesh (PTM), graphite plate and saturated calomel electrode (SCE) were used as the working electrode, the counter electrode and the reference electrode, respectively. The electrodeposition electrolytes contained $NiCl_2·6H_2O$, $(NH_4)_6Mo_7O_{24}·4H_2O$, and $C_6H_5Na_3O_7$. The pH of electrolyte was adjusted to 9.5 by using Na_2CO_3. The electrodeposition was performed at a current density of 100 $mA·cm^{-2}$ for 300 s. As a control, the Ni@PTM and POMs@PTM electrocatalysts were also constructed under the same electrodeposition condition except for without using $(NH_4)_6Mo_7O_{24}·4H_2O$ and $NiCl_2·6H_2O$ respectively.

Physical Characterization: The surface morphologies of the samples were analyzed via field emission scanning electron microscopy (FESEM, Hitachi Regulus-8100) and transmission electron microscopy (TEM, HT7700). High-resolution transmission electron microscopy (HRTEM) images were obtained on Thermo Scientific Talos F200E. The X-ray diffraction (XRD) patterns were recorded on the Rigaku SmartLab with Cu Kα radiation source (λ = 1.5406 Å) in the 2θ range of 10° to 80° with the scanning speed of $5°·min^{-1}$. The surface composition and electronic structure were investigated by X-ray photoelectron spectroscopy (XPS, ESCALAB 250).

Electrochemical measurements: HER performances of the as-prepared electrodes were tested on the electrochemical workstation (Wuhan Corrtest Instruments Corp. Ltd., CS350) by a typical three-electrode setup in 1.0 M KOH aqueous solution. The fabricated electrodes, saturated calomel electrode (SCE) and a graphite rod were as the working electrode, the reference and counter electrodes, respectively. The electrochemical impedance spectroscopy (EIS) was measured with frequencies from 0.1 to 10000 Hz with an AC voltage of 5 mV. Linear sweep voltammetries (LSV) were tested in 1.0 M KOH from 0.05 V to -0.5 V (vs RHE) at a scan rate of 5 mV s^{-1} to evaluate the HER activity of the electrodes. Cyclic voltammetry (CV) was obtained from 0.1 to 0.2 V (vs RHE) with sweep rates of 10, 30, 50, 70, 90 $mV·s^{-1}$. The stability was examined at 10 and 100 $mA·cm^{-2}$.

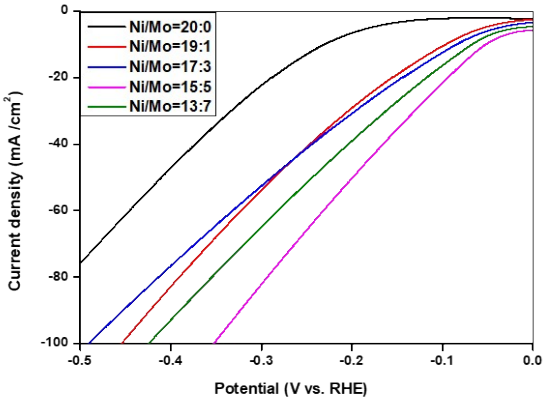

Figure S1. Polarization curves of POMs-Ni@PTM electrocatalysts with different Ni/Mo ratios.

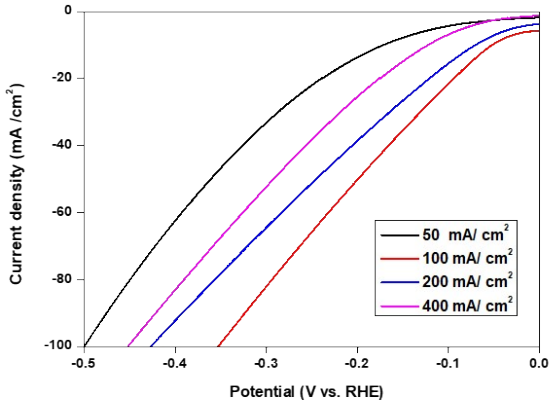

Figure S2. Polarization curves of POMs-Ni@PTM electrocatalysts with different deposition current densities.

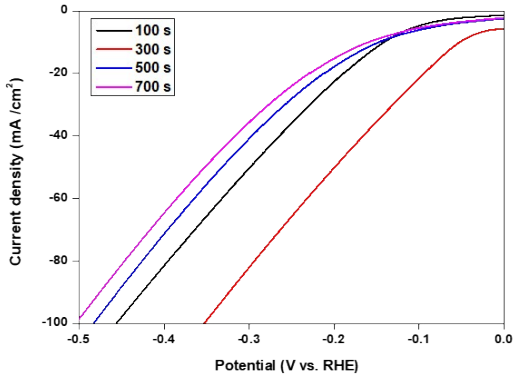

Figure S3. Polarization curves of POMs-Ni@PTM electrocatalysts with different electrodeposition time. Various electrodeposition times have been applied to prepare the POMs-Ni@PTM electrocatalysts, including 100 s (black curve), 300 s (red curve), 500 s (blue curve) and 700 s (pink curve), showing the optimized deposition time to prepare POMs-Ni@PTM electrocatalyst is 300 s.

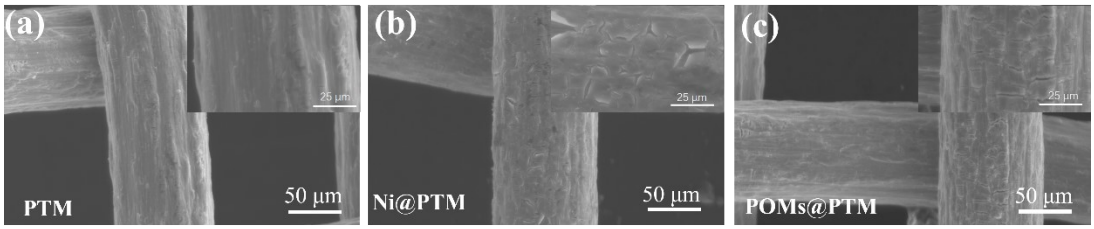

Figure S4. SEM images of controlled samples, including (a) the bared PTM support, (b) the Ni@PTM without POMs, and (c) the POMs@PTM without Ni. The surface of PTM support is smooth, but both of the Ni@PTM and POMs@PTM samples showed thin coating layers on their surface.

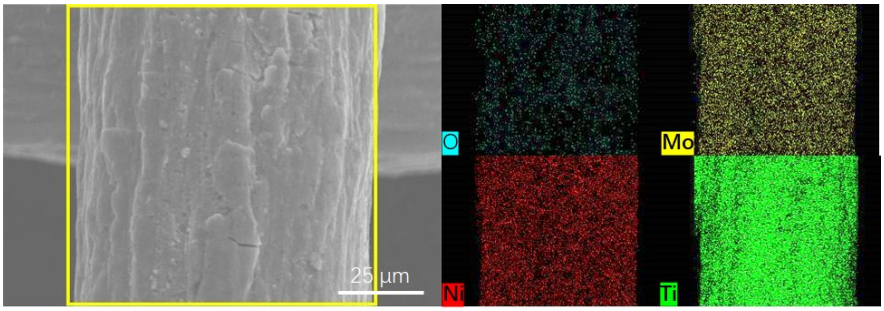

Figure S5. SEM image of POMs-Ni@PTM and the corresponding EDS element mapping of O, Ni, Ti elements.

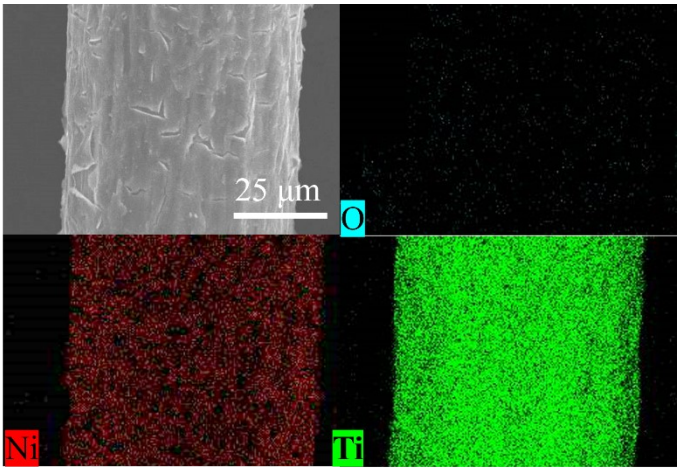

Figure S6. SEM image of Ni@PTM and the corresponding EDS element mapping of O, Ni, Ti elements.

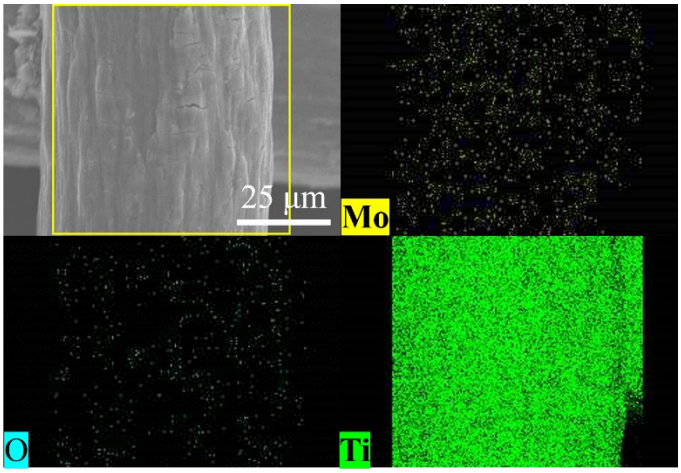

Figure S7. SEM image of POMs@PTM and the corresponding EDS element mapping of O, Mo, Ti elements.

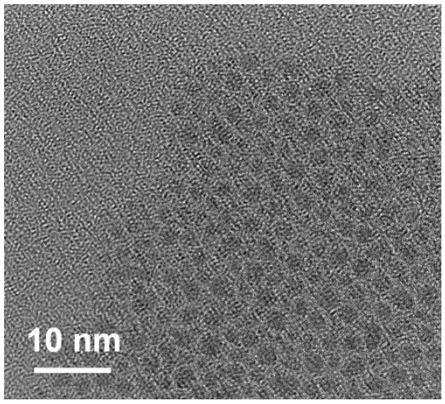

Figure S8. HRTEM images of POMs-Ni@PTM electrocatalyst.

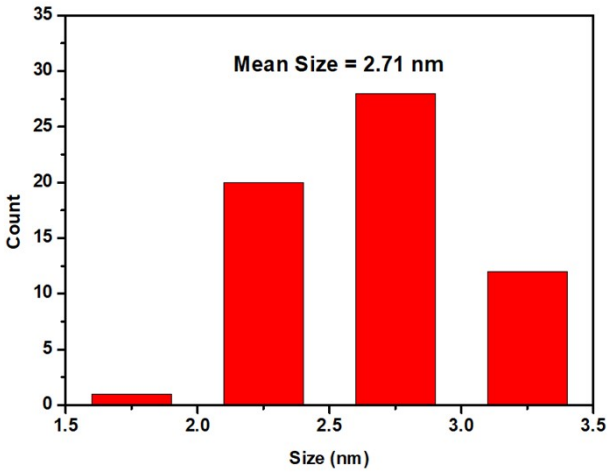

Figure S9. Particle size distribution of quantum dots in Figure S8.

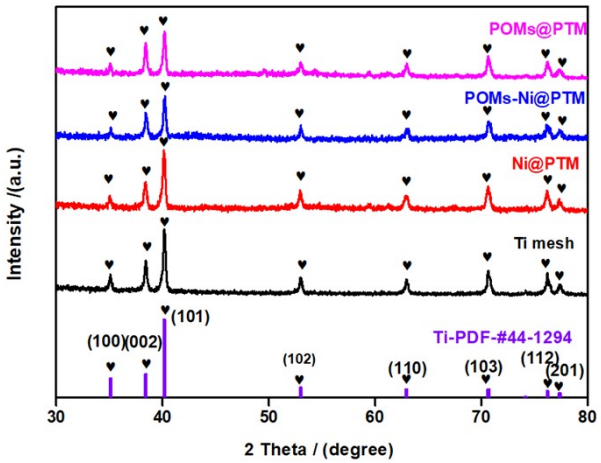

Figure S10. XRD patterns of various samples, including POMs@PTM (pink), POMs-Ni@PTM (blue), Ni@PTM (red), PTM (black).

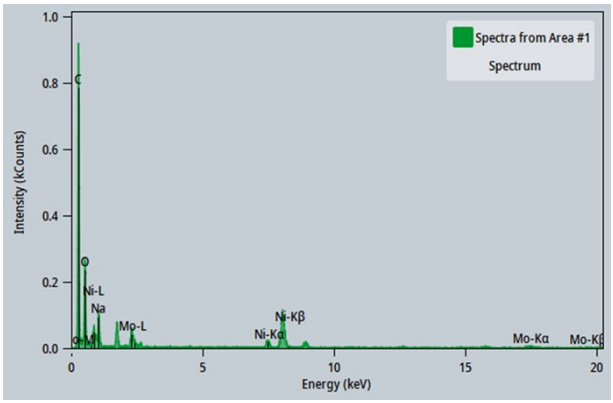

Figure S11. The corresponding EDS intensity profile of POMs-Ni@PTM electrocatalyst in Figure 2g-2i.

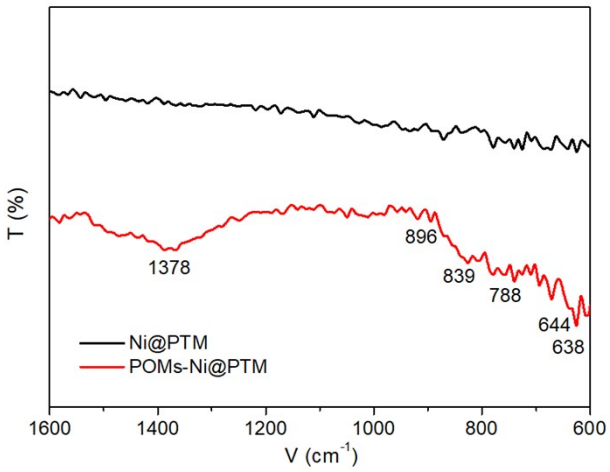

Figure S12. The IR spectra of Ni@PTM (black curve) and POMs-Ni@PTM (red curve) samples.

We further characterize the IR spectrum of POMs-Ni@PTM sample (see Figure S12) to confirm the formation of POMs clusters. The peaks at 896 cm^{-1}, 839 cm^{-1}, 788 cm^{-1}, 644 cm^{-1} and 638 cm^{-1} are characteristic peaks of Mo7 POMs clusters, where peaks of 896 cm^{-1} and 839 cm^{-1} are associated with the Mo=O stretching vibrations, and the peaks at 788 cm^{-1}, 644 cm^{-1} and 638 cm^{-1} are attributed to Mo-O-Mo stretching vibrations [1-3]. The peaks at ~1378 cm^{-1} can be attributed to the vibration of δOH, which may due to the surface water absorption. As a comparison, the Ni@PTM sample shows almost no IR peaks of POMs clusters.

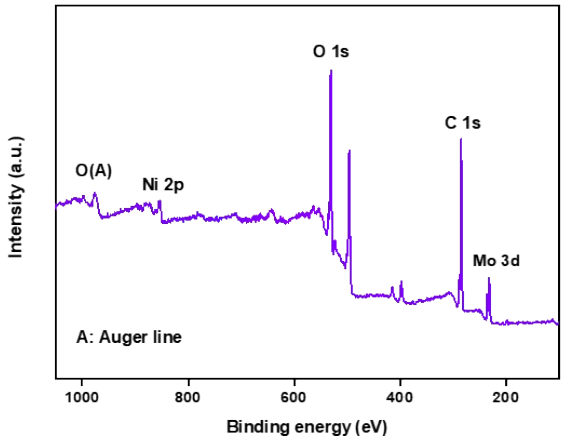

Figure S13. XPS survey spectrum

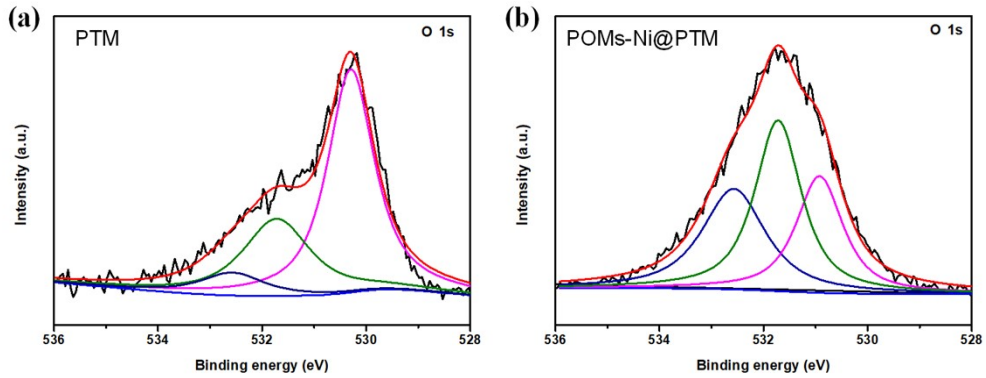

Figure S14. O1s XPS spectra of (a) PTM and (b) POMs-Ni@PTM.

The O1s XPS spectrum of PTM support (see Figure S14a) has been deconvoluted into three peaks at 530.30, 531.72 and 532.57 eV. The peak at 530.30 eV can be assigned to metal-oxygen (M-O) bond. The peaks at 531.72 and 532.57 eV can be assigned to surface hydroxyl oxygen and oxygen in water respectively[4-6]. Compared to PTM, the POMs-Ni@PTM electrocatalyst (see Figure S14b) also shows three similar peak positions (530.92 eV, 531.72 eV and 532.57 eV) in the O1s XPS spectrum. However, the POMs-Ni@PTM electrocatalyst shows much higher peaks of surface hydroxyl and water adsorption, indicating the deposition of POMs-Ni quantum dots can increase the hydrophilia of PTM support.

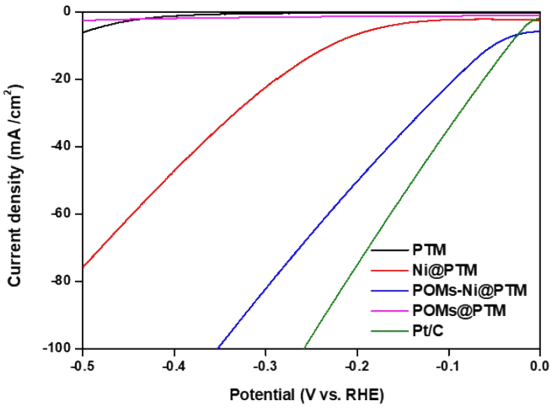

Figure S15. Polarization curves of POMs-Ni@PTM, POMs@PTM, Ni@PTM and 20% Pt/C electrocatalysts (without IR compensation).

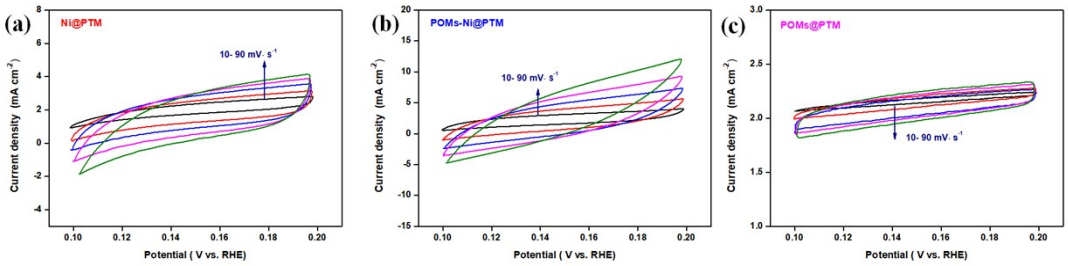

Figure S16. Cdl curves of different samples, (a) Ni@PTM, (b) POMs-Ni@PTM, (c) POMs@PTM

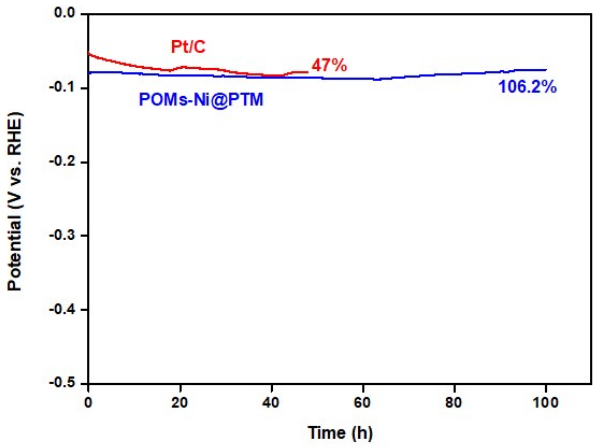

Figure S17. The long-term durability test at a current density of 10 mA·cm^{-2}.

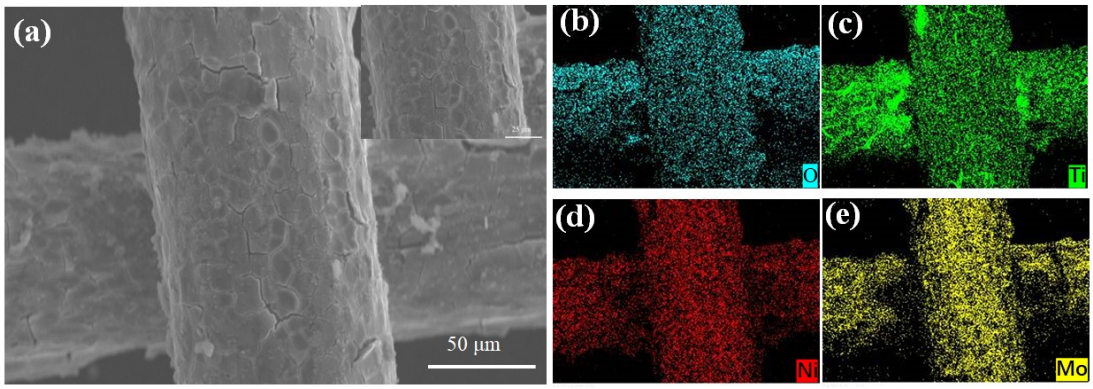

Figure S18. Structure characterizations of POMs-Ni@PTM electrocatalyst after stability test. (a) SEM images. (b-e) EDS element mapping of (b) O, (c) Ti, (d) Ni and (e)Mo elements.

The SEM morphology of POMs-Ni@PTM remains almost unchanged after the long-term durability test at a current density of ~ 100 $mA \cdot cm^{-2}$ for 100 h (Figure S18a). Moreover, the Mo, Ni and O elements are well retained in the POMs-Ni@PTM electrocatalyst after long-term durability testing, as illustrated by the EDX elemental mapping (Figure S18b-18e).

References

1. Y. Huang, Y. Sun, X. Zheng, T. Aoki, B. Pattengale, J. Huang, X. He, W. Bian, S. Younan, N. Williams, J. Hu, J. Ge, N. Pu, X. Yan, X. Pan, L. Zhang, Y. Wei and J. Gu, *Nature Communications*, 2019, **10**, 982.
2. K. Nomiya, T. Takahashi, T. Shirai and M. Miwa, *Polyhedron*, 1987, **6**, 213-218.
3. M. Filowitz, R. K. C. Ho, W. G. Klemperer and W. Shum, *Inorganic Chemistry*, 1979, **18**, 93-103.
4. C. Dong, T. Kou, H. Gao, Z. Peng, Z. Zhang, *Advanced Energy Materials,* 2018, **8**, 1701347.
5. X. Fan, D. Liu, Z. Zhao, J. Li, J. Liu, *Catalysis Today,* 2020*,* **339***,* 67-78.
6. J. Yang, A. G. Baker, H. Liu, W. N. Martens, R. L. Frost, *Journal of Materials Science,* 2010, **45**, 6574-6585.